AB

KEK Preprint 96-152
HUPD-9621
KOBE HEP 96-04
KUNS-1426
OULNS 96-04
December 1996
H

$D^{*\pm}$ Inclusive Production in Two-photon Process at $\sqrt{s}$ = 58 GeV in TRISTAN

VENUS Collaboration

SW9708

Submitted to Z. Phys. C

National Laboratory for High Energy Physics, 1996

KEK Reports are available from:

Technical Information & Library
National Laboratory for High Energy Physics
1-1 Oho, Tsukuba-shi
Ibaraki-ken, 305
JAPAN

Phone: 0298-64-5136
Telex: 3652-534 (Domestic)
(0)3652-534 (International)
Fax: 0298-64-4604
Cable: KEK OHO
E-mail: Library@kekvax.kek.jp (Internet Address)
Internet: http://www.kek.jp

$D^{*\pm}$ inclusive production in two-photon process at $\sqrt{s} = 58$ GeV in TRISTAN

VENUS Collaboration

H.Ohyama[a], K.Abe[b], K.Amako[c], Y.Arai[c], Y.Asano[d], M.Chiba[e], Y.Chiba[f], M.Daigo[g], M.Fukawa[c,1], Y.Fukushima[c], J.Haba[c], H.Hamasaki[d], H.Hanai[h], Y.Hemmi[i], M.Higuchi[j], T.Hirose[e], Y.Homma[k], N.Ishihara[c], Y.Iwata[ℓ], J.Kanzaki[c], R.Kikuchi[i], T.Kondo[c], T.T.Korhonen[c,m,2], H.Kurashige[i], E.K.Matsuda[n], T.Matsui[c], K.Miyake[i], S.Mori[d], Y.Nagashima[h], Y.Nakagawa[o,3], T.Nakamura[p*], I.Nakano[n], S.Odaka[c], K.Ogawa[c*], T.Ohama[c], T.Ohsugi[ℓ], K.Okabe[n], A.Okamoto[i], A.Ono[q], J.Pennanen[c,m], H.Sakamoto[i], M.Sakuda[c], M.Sato[j], N.Sato[c], M.Shioden[r], J.Shirai[c], T.Sumiyoshi[c], Y.Takada[d], F.Takasaki[c], M.Takita[h], N.Tamura[s], D.Tatsumi[h], K.Tobimatsu[t], T.Tsuboyama[c], S.Uehara[c], Y.Unno[c], T.Watanabe[u], Y.Watase[c], F.Yabuki[e], Y.Yamada[c], T.Yamagata[o], Y.Yonezawa[v], H.Yoshida[w] and K.Yusa[d]

[a] Hiroshima National College of Maritime Technology, Higashino-cho, Hiroshima-ken 725-02, Japan
[b] Department of Physics, Tohoku University, Aoba-ku, Sendai 980, Japan
[c] KEK, National Laboratory for High Energy Physics, Tsukuba 305, Japan
[d] Institute of Applied Physics, University of Tsukuba, Tsukuba 305, Japan
[e] Department of Physics, Tokyo Metropolitan University, Hachioji 192-03, Japan
[f] Yasuda Women's Junior College, Asa-Minami-ku, Hiroshima 731-01, Japan
[g] Faculty of Economics, Toyama University, Toyama 930, Japan
[h] Department of Physics, Osaka University, Toyonaka 560, Japan
[i] Department of Physics, Kyoto University, Sakyo-ku, Kyoto 606, Japan
[j] Department of Applied Physics, Tohoku-Gakuin University, Tagajo 985, Japan
[k] Department of Electorical and Electronics Engineering, Kobe University,Nada-ku,Kobe 657, Japan
[ℓ] Department of Physics, Hiroshima University, Higashi-Hiroshima 739, Japan
[m] Research Institute for High Energy Physics, University of Helsinki, Helsinki FIN-00014, Finland
[n] Department of Physics, Okayama University, Okayama 700, Japan
[o] Division of Natural Sciences, International Christian University, Mitaka 181 Japan
[p] Faculty of Engineering, Miyazaki University, Miyazaki 889-01, Japan
[q] Faculty of Cross-Cultural Studies, Kobe University, Nada-ku, Kobe 657, Japan
[r] Department of Electronic and Computer Engineering, Ibaraki College of Technology, Hitachinaka 312, Japan
[s] Department of Physics, Niigata University, Niigata 950-21, Japan
[t] Center for Information Science, Kogakuin University, Shinjuku-ku, Tokyo 163-91, Japan
[u] Department of Physics, Kogakuin University, Hachioji, Tokyo 192, Japan
[v] Tsukuba College of Technology, Tsukuba 305, Japan
[w] Naruto University of Education, Naruto 772, Japan

* Deceased
[1] Present address: Naruto University of Education, Naruto 772, Japan

[2] Present address: Accelerator Division, KEK, National Laboratory for High Energy Physics, Tsukuba 305, Japan
[3] Present address: Faculty of Science, Ehime University, Matsuyama 790, Japan

Abstract

Using the VENUS detector at TRISTAN we have investigated the charm-quark production by detecting $D^{*\pm}$ mesons in the two-photon process of e^+e^- collisions. The study has confirmed that the charm-quark production rate is larger than that predicted from direct $c\bar{c}$ production alone. The distribution of the transverse momentum of the $D^{*\pm}$ mesons and the forward energy flow associated with the $D^{*\pm}$ production suggest that the main part of the observed excess comes from the contribution of a resolved photon process.

1 Introduction

The charm-quark production in two-photon processes is suitable for studying the quantum chromo-dynamical (QCD) structure of the photon. The contribution from the non-perturbative soft process for charm-quark production is expected to be small, compared to that from light-quark production, since the charm-quark mass is significantly larger than the typical QCD energy scale. Several experimental studies concerning this process have been reported by experimental groups at PEP[1], PETRA[2, 3] TRISTAN[4, 5, 6], and LEP[7]. From these studies it has become clear that the production cross section is significantly larger than the theoretical prediction which assumes a naive direct pair-production process, $\gamma\gamma \to c\bar{c}$. The excess is considered to come from the resolved photon process[8], where the hadronic nature of the photon allows one of the photons to be resolved into a gluon and hadronic remnants (once resolved photon process); the gluon interacts with the other incoming photon to create a pair of charm quarks, $g\gamma \to c\bar{c}$.

In this aspect, charm-quark production in the two-photon process represents a good place to measure the gluonic structure of the photon[9]. However, the data accumulated so far are not sufficient to discuss the gluonic structure quantitatively, and many more measurements are needed.

In this report we present experimental results concerning the production of $D^{*\pm}$ mesons in the two-photon process using the VENUS detector at the TRISTAN e^+e^- collider. The analysis is based on data accumulated at center-of-mass energies of between 57.6 and 59.7 GeV with an average value of 58.0 GeV for an integrated luminosity of 206 pb^{-1}. The $D^{*\pm}$ mesons are reconstructed through the decay branches, $D^{*\pm} \to D^0(\bar{D}^0)\pi^\pm$, followed by $D^0(\bar{D}^0) \to K^\mp\pi^\pm$ or $K^\mp\pi^\pm\pi^\mp\pi^\pm$. The signal events are enriched by identifying kaons in the final state by means of a time-of-flight measurement. The $D^{*\pm}$ mesons are selected by the mass-difference method, where a small mass difference between $D^{*\pm}$ and D^0 enables us to discriminate the $D^{*\pm}$ signal from combinatorial backgrounds.

The results have been compared with the theoretical predictions of the direct process and that of the resolved photon process. The observed transverse momentum spectrum of $D^{*\pm}$ mesons and the forward energy flow associated with the $D^{*\pm}$ production have been studied, where the latter is thought to be a distinctive signature of the resolved photon process.

2 Experimental Procedure

2.1 VENUS detector

The VENUS detector was a general-purpose solenoid detector operated at one of the four interaction points of TRISTAN. It had been stably operated without any major problem since the TRISTAN accelerator was commissioned in November, 1986, until the end of the experiment in May, 1995. An overview of the VENUS detector can be found elsewhere [10]. We describe here only those features relevant to the present analysis.

The charged particles were detected by a central drift chamber (CDC)[11] placed inside of a 0.75 T axial magnetic field of a superconducting solenoid. The CDC detector was a conventional multi-wire drift chamber of 3 m in length, having 20 axial and 9 stereo layers. The CDC covered a polar angular region of $|\cos\theta| < 0.85$. The resolution of the transverse momentum measured by the CDC is given by $\sigma_{p_t}^{CDC}/p_t = \sqrt{(1.3\%)^2 + (0.8\% \times p_t)^2}$, where p_t is in units of GeV/c. Tracks having a transverse momentum larger than 100 MeV/c were detected by the CDC and used for the analysis. The TOF counters[12] were located at 1.64 m apart from the e^+e^- beam line. They were used to distinguish kaons from pions. The particles having a transverse momentum larger than 200 MeV/c and emitted in the region of $|\cos\theta| < 0.81$ were detected with the TOF counters. Since the counters had a time resolution of 250 ps, the $K^\pm$ having a momentum less than 1.0 GeV/c was clearly distinguished from $\pi^\pm$. For particles having a momentum of between 1.0 and 1.5 GeV/c, the TOF counters could still help to identify kaons. A scatter plot for the momenta versus the measured mass reconstructed by the TOF information is shown in Fig.1 for charged tracks in collected events.

The electromagnetic calorimeters of the lead glass (LG)[13] and liquid Ar (LA)[14] were used to measure the total visible energy together with the CDC to separate the two-photon process from e^+e^- annihilation events. The transition region between the forward LA and the barrel LG calorimeters was overlapped to attain a hermetic calorimeter coverage down to $|\cos\theta| = 0.990$. The LA was also used for detecting recoil electrons and the remnant energy flow associated with the resolved photon process. The energy resolutions of the LG and LA calorimeters were $\sigma_E^{LG}/E = 2.5\% + 7.0\%/\sqrt{E}$ and $\sigma_E^{LA}/E = 1.6\% + 10.2\%/\sqrt{E}$, respectively, where E is in units of GeV. The LG and LA calorimeters were safely sensitive to energy deposits down to 100 MeV and 200 MeV, respectively.

The events collected and analyzed here were taken with a track-recognition trigger in the track finder circuits[15] and with energy deposited in each segment of the LG calorimeter. The performance of each detector mentioned above and the trigger conditions are implemented in a Monte-Carlo simulation to calculate the number of events expected, and to estimate the detection efficiencies of the two-photon events.

2.2 Event selection

Selection of two-photon events

We required that neither of the scattered electrons are detected so as to study the properties of quasi-real photons (hereafter we call anti-tagging condition). The hadron production events in the two-photon process are selected by imposing the criteria of a total visible energy of $E_{\rm vis} \leq 20$ GeV and the number of good charged tracks of $N_{\rm good} \geq 4$ to the sample events which have two or

more charged tracks with $p_t > 0.2$ GeV/c. The good charged tracks are defined by the following criteria: $|r_{\rm min}| < 1.0$ cm, $|z_{\rm min}| < 6.0$ cm, $p_t > 0.1$GeV/c, and $|\cos\theta| \leq 0.85$, where $r_{\rm min}$ ($z_{\rm min}$) stands for the radial distance (z distance) of the closest approach to the interaction point of the track in the $r\varphi$ plane (in the z-coordinate). The total visible energy ($E_{\rm vis}$) is defined as the sum of the absolute momenta of the charged particles and of the total energies deposited in the calorimeters, LG and LA. The distribution of the total visible energy is shown in Fig.2, which includes a part of the sample before the $E_{\rm vis}$ and $N_{\rm good}$ cuts are applied. The $E_{\rm vis}$ cut rejects those events in which the recoil electron is detected as well as those coming from e^+e^- annihilation process.

Kaon enriched samples

$D^{*\pm}$ mesons are searched in kaon-enriched samples in which at least one candidate of a charged track is found to be a kaon candidate in the events survived by the above selection criteria. The $K^{\pm}$ candidates are selected among those tracks having $p_t \geq 0.3$ GeV/c and should satisfy the following time-of-flight condition:

$$\exp\left[-\frac{1}{2}\left\{\frac{TOF_{\rm measured} - TOF_{\rm expected}}{\sigma_{\rm TOF}}\right\}^2\right] > 0.01,$$

where $TOF_{\rm measured}$ is the time of flight measured by the TOF counters and $TOF_{\rm expected}$ is the value calculated from the corresponding path length and the measured momentum, assuming the kaon mass. The error $\sigma_{\rm TOF}$ is given by a quadratic sum of the intrinsic time resolution of the TOF counters and an error in the time derived from the uncertainty in the momentum measurement by the CDC.

Selection of $D^{*\pm}$ candidates

A mass-difference method is used to identify $D^{*\pm}$ mesons. The decay $D^{*\pm} \rightarrow D^0(\bar{D}^0) + \pi^{\pm}$ has a small Q value of 5.9 MeV, so that the mass difference between $D^{*\pm}$ and D^0 (D^0 includes $\bar{D}^0$ hereafter) is expected to make a sharp peak at around 145.5 MeV/c^2, just above the pion production threshold. In this study the D^0 mesons are reconstructed in its decay branches to $K^{\mp}\pi^{\pm}$ and $K^{\mp}\pi^{\pm}\pi^{\mp}\pi^{\pm}$. The identified kaon tracks are combined with other tracks, and the invariant mass of those tracks are evaluated, where we assume any other good track to be a pion. The mass bands imposed to select the D^0 candidates are $1.79 < M_{K\pi} < 1.93$ GeV/c^2 for $K^{\mp}\pi^{\pm}$ and $1.81 < M_{K\pi\pi\pi} < 1.91$ GeV/c^2 for $K^{\mp}\pi^{\pm}\pi^{\mp}\pi^{\pm}$ branches, respectively. Since most of the $K^{\mp}\pi^{\pm}\pi^{\mp}\pi^{\pm}$ events come through the $K^{\mp}\pi^{\pm}\rho^0$ channel in the decays of D^0, we require invariant mass of one combination in opposite-charged pions to be within $0.67 < M_{\pi^+\pi^-} < 0.87$ GeV/c^2, in order to improve the signal-to-noise ratio.

Although in the D^0 rest frame the decay kaons are expected to be emitted isotropically, the observed kaons peak at around the D^0 production direction. This suggests that most of forward kaons are backgrounds. To improve the signal-to-noise ratio, we impose the cut $|\cos\theta^*_K| < 0.9$ ($|\cos\theta^*_K| < 0.7$) for the $K^{\mp}\pi^{\pm}$ ($K^{\mp}\pi^{\pm}\pi^{\mp}\pi^{\pm}$) branch, where θ^*_K is the kaon emission angle in the D^0 rest frame with respect to the D^0 production direction. For those events having D^0 candidates, the mass difference (ΔM) of $D^{*\pm}$ and D^0 is calculated for every combination of the D^0 candidate and the remaining pion track. The ΔM distributions for the $K^{\mp}\pi^{\pm}$ and $K^{\mp}\pi^{\pm}\pi^{\mp}\pi^{\pm}$ branches are shown in Figs.3(a) and (b), respectively. The $D^{*\pm}$ signal peaks in a ΔM band of $0.1415 < \Delta M < 0.1495$ GeV/c^2 for both the $K^{\mp}\pi^{\pm}$ and $K^{\mp}\pi^{\pm}\pi^{\mp}\pi^{\pm}$ branches. There is one (two) event in which two candidates of the $D^{*\pm}$, contained in the above mass band, share an identical $K^{\mp}$ track in the $K^{\mp}\pi^{\pm}$ ($K^{\mp}\pi^{\pm}\pi^{\mp}\pi^{\pm}$) branch. We chose the combination of the smaller ΔM in such a case. The number of selected $D^{*\pm}$ candidates is 29 and 26 for the branches of $K^{\mp}\pi^{\pm}$ and $K^{\mp}\pi^{\pm}\pi^{\mp}\pi^{\pm}$, respectively. We have found no events having two or more independent $D^{*\pm}$ meson candidates in an event.

The contribution of combinatorial background is estimated from the ΔM distribution. A third-order polynomial function of ΔM, which vanishes at $\Delta M = m_{\pi^\pm}$, is fitted to the distribution in the $0.15 < \Delta M < 0.30$ GeV/c^2 region. The shape of the background distribution is also checked by control samples which fall in the off-D^0 mass region, $2.0 < M_{K\pi} < 2.5$ GeV/c^2. The ΔM distribution of the control samples does not have any peculiar structure in the signal region, as shown in Fig.4. We do not use a wrong sign combination of $\pi^\pm$ for the reconstruction of $D^{*\pm}$ to see the background shape, because it has a chance to include real $D^{*\pm}$ particles due to the misidentification of a kaon. The estimated numbers of combinatorial backgrounds in the signal region are 2.5 ± 1.6 and 8.7 ± 2.9 for the $K^\mp\pi^\pm$ and $K^\mp\pi^\pm\pi^\mp\pi^\pm$ branches, respectively. The attached errors are only statistical.

The background $D^{*\pm}$ from the e^+e^- annihilation process is estimated by a Monte-Carlo simulator to be 1.0 ± 0.6 and 0.7 ± 0.5 particles for the $K^\mp\pi^\pm$ and $K^\mp\pi^\pm\pi^\mp\pi^\pm$ branches, respectively. By subtracting the backgrounds estimated above, the number of $D^{*\pm}$ mesons observed are:

$$N_{\rm observed} = 25.5 \pm 5.4 \text{ for } D^{*\pm} \to K^\mp\pi^\pm\pi^\pm,$$
$$N_{\rm observed} = 16.6 \pm 5.1 \text{ for } D^{*\pm} \to K^\mp\pi^\pm\pi^\mp\pi^\pm\pi^\pm.$$

2.3 Monte-Carlo Expectations

We have calculated the numbers of $D^{*\pm}$ expected from the direct and once resolved photon processes by making use of Monte-Carlo (MC) event generators. The direct-process events are generated by a program developed by Berends, Daverveldt and Kleiss [16], which includes all relevant α^4 diagrams in the tree level. The charm-quark mass of 1.6 GeV/c^2 is used in the calculation. Event generation for the once resolved photon process is carried out using the PYTHIA5.6 program[17] with default parameters and the LAC1 parametrization[18] for the gluon density function in the photon. The gluon density function with the LAC1 parameters showed reasonable agreement with the experimental data in the previous TRISTAN experiments for charm-quark production[4, 5, 6]. The contribution from the twice resolved photon processes and one from the $b\bar{b}$ production in the two-photon processes are estimated to be less than 2%, and thus neglected. The program JETSET7.3[17] is used for the quark-fragmentation process. The branching fraction of the charm (or anti-charm) quark to make the D^{*+} (or D^{*-}) meson is set to be $21.5 \pm 1.5\%$ by averaging over available data [19, 20]. The decay fraction of $D^{*\pm} \to D^0\pi^\pm$ is taken to be $68.1 \pm 1.6\%$ [21]. The decay fractions of $D^0 \to K^-\pi^+$ and $D^0 \to K^-\pi^+\pi^-\pi^+$ are set to be $3.84 \pm 0.13\%$ and $7.5 \pm 0.4\%$ [21], respectively.

In calculations of the expectation values, a systematic error in the choice of the charm quark mass is estimated to be 17% and 15% for the direct and once resolved photon processes, respectively, where we vary the charm mass from 1.4 to 1.75 GeV/c^2. For the once resolved photon process, in addition, an error in the assignment of energy scale (Q^2) for photon-gluon fusion is estimated to be 20% by replacing the default assignment of the transverse-mass squared for the charm quark in PYTHIA7.3 ($Q^2 = (m_{Tc}^2 + m_{T\bar{c}}^2)/2$) with the total-energy squared for the photon-gluon system ($Q^2 = W_{g\gamma}^2$). A next-to-leading-order QCD correction to the direct process is estimated to be $30 \pm 10\%$ [9]. The generated events are passed through the detector simulator of the VENUS detector with the trigger conditions imposed on the analyzed data.

By taking account of the errors and the QCD correction to the direct process discussed above, the number of $D^{*\pm}$ expected for the present experimental conditions are, for the $D^{*\pm} \to$

$D^0\pi^\pm$, $D^0 \to K^\mp\pi^\pm$ branch:

$$\begin{aligned} N_{\rm direct} &= 11.4 \pm 2.4 \text{ (before QCD correction)}, \\ N_{\rm direct} &= 14.8 \pm 3.5 \text{ (after QCD correction)}, \\ N_{\rm resolved} &= 6.3 \pm 2.0 \text{ (with LAC1 parameters)}, \end{aligned}$$

where $N_{\rm direct}$ ($N_{\rm resolved}$) denotes the expected number of $D^{*\pm}$ mesons from the direct process (the once resolved photon process). For the $D^{*\pm} \to D^0\pi^\pm$, $D^0 \to K^\mp\pi^\pm\pi^\mp\pi^\pm$ branch, the numbers expected are:

$$\begin{aligned} N_{\rm direct} &= 5.6 \pm 1.5 \text{ (before QCD correction)}, \\ N_{\rm direct} &= 7.2 \pm 2.1 \text{ (after QCD correction)}, \\ N_{\rm resolved} &= 2.7 \pm 1.0 \text{ (with LAC1 parameters)}. \end{aligned}$$

The sum of the contribution from the direct process with the QCD correction and that from the resolved photon process is expected to be 21.1 ± 5.3 and 10.0 ± 2.8 for the $D^{*\pm} \to K^\mp\pi^\pm\pi^\pm$ and $D^{*\pm} \to K^\mp\pi^\pm\pi^\mp\pi^\pm\pi^\pm$ branches, respectively.

If the DG parameter set [22] for the resolved photon process is assumed in comparison with the LAC1, the number of $D^{*\pm}$ mesons for the $D^{*\pm} \to K^\mp\pi^\pm\pi^\pm$ branch is predicted to be 2.1 ± 0.7.

3 Result and Discussion

The number of $D^{*\pm}$ observed for $D^{*\pm} \to K^\mp\pi^\pm\pi^\pm$ and $D^{*\pm} \to K^\mp\pi^\pm\pi^\mp\pi^\pm\pi^\pm$ branches are 25.5 ± 5.4 and 16.6 ± 5.1, which should be compared with 14.8 ± 3.5 and 7.2 ± 2.1 particles, respectively, predicted through the direct $c\bar{c}$ production with the QCD correction. The observed number is about two-times larger than the prediction, which corresponds to the combined significance of a 2.2 standard deviation (σ) away from the prediction of the direct process with the QCD correction. Although the sum of the contribution from the direct process with the QCD correction and that from the resolved photon process with the LAC1 parameter set falls within one standard deviation from the observed number, twice the yield from the resolved photon contribution with the LAC1 parameter set can fit much better to the data. This result seems to be consistent with those by other measurements at the TRISTAN[4, 5, 6], although different kinematical conditions imposed in the event selections make a direct comparison among them difficult.

We have studied the differential distribution of $D^{*\pm}$ production to see further evidence of the resolved photon contribution. Figures 5(a) and (b) show the transverse-momentum (p_t) distributions of the $D^{*\pm}$ mesons observed in the decay branches of $K^\mp\pi^\pm\pi^\pm$ and $K^\mp\pi^\pm\pi^\mp\pi^\pm\pi^\pm$, respectively, together with the expectations from the MC calculations shown by histograms.

A forward jet associated with $D^{*\pm}$ production is one of the characteristic features of the resolved photon process. The gluon component in the photon is absorbed by a charm quark in the charm production in the resolved photon process. The remnant component of the photon makes a forward jet which hits the forward calorimeters. Figures 6(a) and (b) show the

distributions of the forward energy deposited in the LA calorimeters associated with the $D^{*\pm}$ production for the two branches, respectively, together with the MC expectations (histograms). We define the forward energy flow to be the larger one of the deposited energies on the two sides of LA in the angular regions of $|\cos\theta| > 0.9$. The observed distributions of the p_t and the forward energy flow include the backgrounds (estimated in Sect.3 to be 3.5 ± 1.7 and 9.4 ± 2.9 for (a) and (b), respectively), while the MC distributions do not.

In the p_t distribution of the observed $D^{*\pm}$, the excess at low-p_t requires a greater contribution from the resolved photon. In addition, the spectrum of the associated forward energy flow is clearly in favor of increasing the contribution of the resolved photon process, which has a remnant jet, thus giving a higher forward energy flow.

We have evaluated the $D^{*\pm}$ production cross section in the kinematical region of $1.0 \leq p_t(D^*) \leq 6.0$ GeV/c and $|\cos\theta(D^*)| \leq 0.7$, with the scattered electrons of $|\cos\theta_{e+}| > 0.990$ and $|\cos\theta_{e-}| > 0.990$ at the center-of-mass energy of e^+e^- being 58 GeV, where $\theta_{e-}(\theta_{e+})$, $p_t(D^*)$ and $\theta(D^*)$ denote the scattered angle of the incident electron(positron), transverse momentum and production angle of the $D^{*\pm}$ with respect to the beam direction, respectively. The detection efficiency of $D^{*\pm}$ in the above kinematical range in the $D^{*\pm} \to K^{\mp}\pi^{\pm}\pi^{\pm}$ branch was estimated for both the direct and resolved photon processes to be $20.3 \pm 2.2\%$ and $14.4 \pm 2.1\%$, respectively. For an evaluation of the average efficiency, we assume that 45% of the observed $D^{*\pm}$ comes from the direct process and the remaining part from the resolved photon process with the LAC1 parameter set. The cross section for the above acceptance is obtained to be $\sigma = 27.7 \pm 5.8 \pm 3.6$ pb. The first-term error is statistical and the second systematic.

4 Conclusions

We have measured the $D^{*\pm}$ production in the two-photon process using a mass-difference method. The observed number of $D^{*\pm}$ is compared with the number expected from the direct and resolved photon processes. The combined significance of the $D^{*\pm}$ particles excess in the $K^{\mp}\pi^{\pm}\pi^{\pm}$ and $K^{\mp}\pi^{\pm}\pi^{\mp}\pi^{\pm}\pi^{\pm}$ branches is 2.2σ over the number predicted by the direct process with the next-to-leading-order QCD correction. Though the statistical significance of this excess is not striking, the event excess is in favor of increasing the resolved photon contribution more than predicted by the LAC1 parameter set. The transverse momentum of the observed $D^{*\pm}$ and the associated forward energy flow also strongly support the interpretation that the excess comes from the contribution of the resolved photon process. The data in this experiment are, however, still not sufficient to determine a favorable model or a parameter set from various models of the resolved photon. The $D^{*\pm}$ production cross section is found to be $27.7 \pm 5.8 \pm 3.6$ pb within the kinematical ranges of $1.0 \leq p_t(D^*) \leq 6.0$ GeV/c and $|\cos\theta(D^*)| \leq 0.7$ under the anti-tagging condition $|\cos\theta_{e^{\pm}}| > 0.990$ from analyses of $D^{*\pm} \to K^{\mp}\pi^{\pm}\pi^{\pm}$ branch.

Acknowledgements
We would like to thank TRISTAN accelerator crew for their excellent operation of the accelerator. We acknowledge the outstanding support of the technical staff at KEK and collaboration institutes. The authors, H.O. and T.O., would like to express special thanks to Prof. Y.Sumi for his continuous encouragement during this work.

References

[1] TPC/Two-Gamma Collab., M.Alston-Garnjost *et al.*, Phys. Lett. **B252**(1990)499.

[2] JADE Collab., W.Bartel *et al.*, Phys. Lett. **B184**(1987)288.

[3] TASSO Collab., W.Braunschweig *et al.*, Z. Phys. **C47**(1990)499.

[4] TOPAZ Collab., R.Enomoto *et al.*, Phys. Rev. D **50** (1994)1879; TOPAZ Collab., R.Enomoto *et al.*, Phys. Lett. **B328**(1994)535; TOPAZ Collab., M.Iwasaki *et al.*, Phys. Lett. **B341** (1994)99.

[5] VENUS Collab., S.Uehara *et al.*, Z. Phys. **C63**(1994)213.

[6] AMY Collab., T.Aso *et al.*, Phys. Lett. **B363**(1995)249; AMY Collab., N.Takashimizu *et al.*, Phys. Lett. **B381**(1996)372.

[7] ALEPH Collab., D.Buskulic *et al.*, Phys Lett **B355**(1995)595.

[8] M.Dress and R.M.Godbole, Nucl. Phys. **B339**(1990)355; M.Dress ans R.M.Godbole, Pramana J. Phys. **41**(1993)83, preprint BU-TH-92/5 (1992); M.Dress ans R.M.Godbole, preprint BU-TH-95/2 (1995).

[9] M.Dress, M.Krämer, J.Zunft and P.M.Zerwas, Phys. Lett. **B306** (1993)371.

[10] VENUS Collab., K.Abe et al., Phys. Lett. **B232**(1989)431; VENUS Collab., K.Abe et al., Z. Phys. C **45**(1989)175; VENUS Collab., A.Taketani et al., Phys. Lett. **B234**(1990)202.

[11] R.Arai *et al.*, Nucl. Instr. Meth. **A217**(1983)181.

[12] Y.Hemmi *et al.*, Jpn. J. Appl. Phys. **26**(1987)982.

[13] K.Ogawa *et al.*, Nucl. Instr. Meth. **A228**(1985)309; K.Ogawa *et al.*, Nucl. Instr. Meth. **A238**(1985)328; K.Ogawa *et al.*, Nucl. Instr. Meth. **A243**(1986)358; T.Sumiyoshi *et al.*, Nucl. Instr. Meth. **A271**(1988)432.

[14] Y.Fukushima *et al.*, IEEE Trans. Nucl. Sci. **36**(1989)670.

[15] T.Ohsugi *et al.*, Nucl. Instr. Meth. **A270**(1988)319.

[16] P.H.Daverveldt, F.A.Berends and R.Kleiss, Nucl. Phys. **B253**(1985)441 and Comp. Phys. Comm. **40**(1986)285.

[17] T.Sjöstrand. preprint CERN-TH. 6488/92 (1992).

[18] H.Abramowicz, K.Charchula and A.Levy, Phys. Lett. **B269**(1991)458.

[19] M.Sakuda, Nuovo Cim. **107A**(1994)2389.

[20] CLEO Collab., D.Bortoletto *et al.*, Phys. Rev. **D37**(1988)1719; ARGUS Collab., H.Albrecht *et al.*, Z. Phys. **C52**(1991)353; HRS Collab., P.Baringer *et al.*, Phys. Lett. **B206**(1988)551; ALEPH Collab., D.Decamp *et al.*, Phys. Lett. **B266**(1991)218; VENUS Collab., F.Hinode *et al.*, Phys. Lett. **B313**(1992)245; TOPAZ Collab., E.Nakano *et al.*, Phys. Lett. **B314**(1992)471.

[21] Particle Data Group, L. Montanet *et al.*, Phys. Rev. **D50**(1994)1173 and 1995 off-year partial update for the 1996 edition available on the PDG WWW pages (URL: http://pdg.lbl.gov/).

[22] M.Dress and K.Grassie, Z.Phys. **C28**(1985)451.

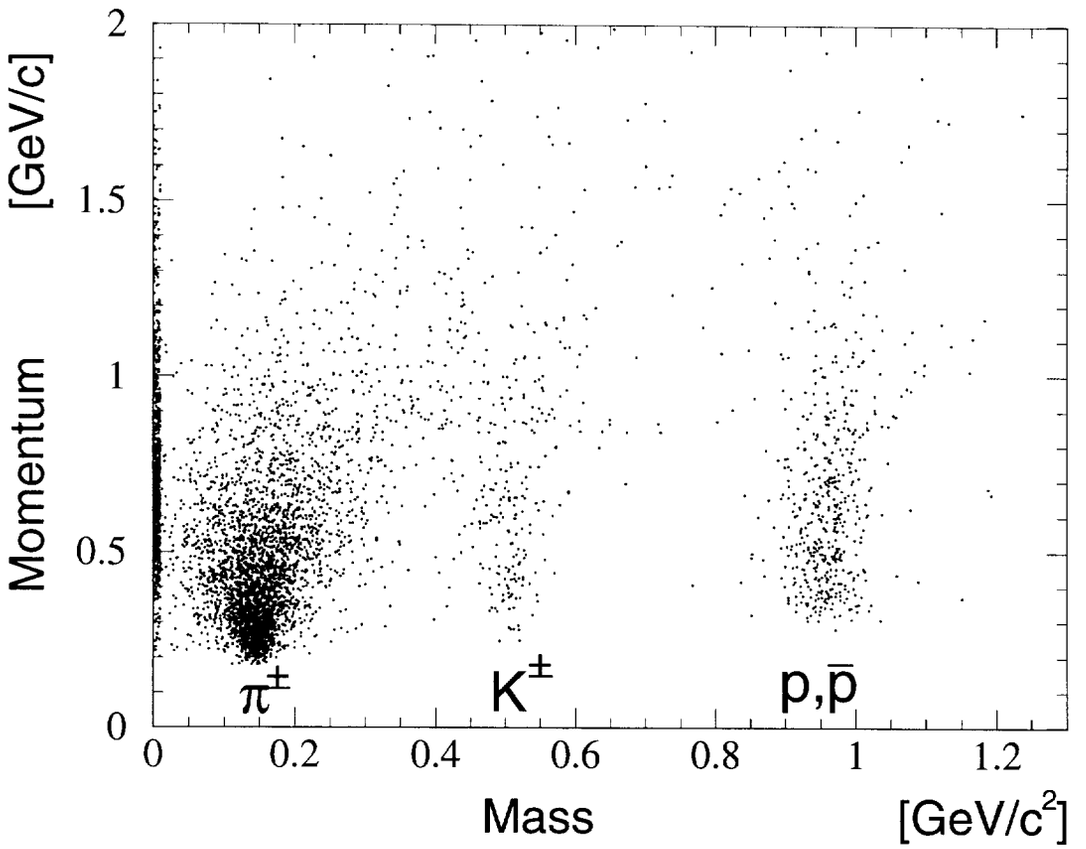

Figure 1: Scatter plot of the momentum vs measured mass based on the TOF information

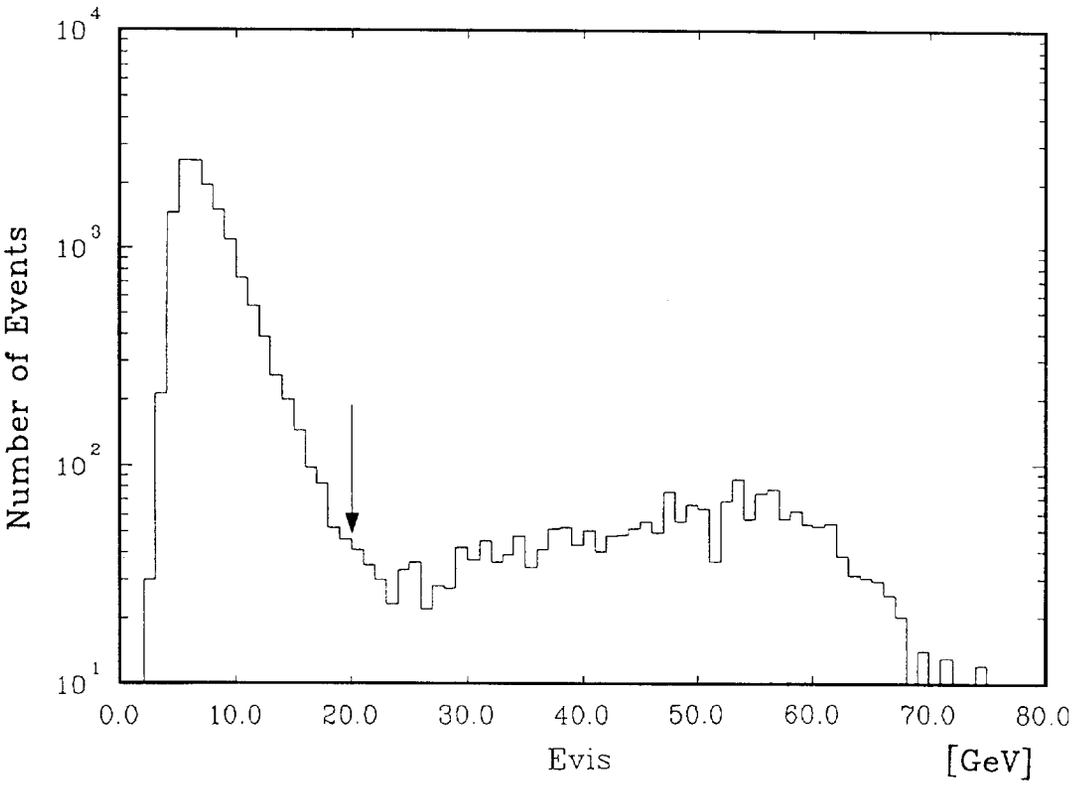

Figure 2: Total visible energy distribution. The arrow shows the cut to select events in the two-photon processes

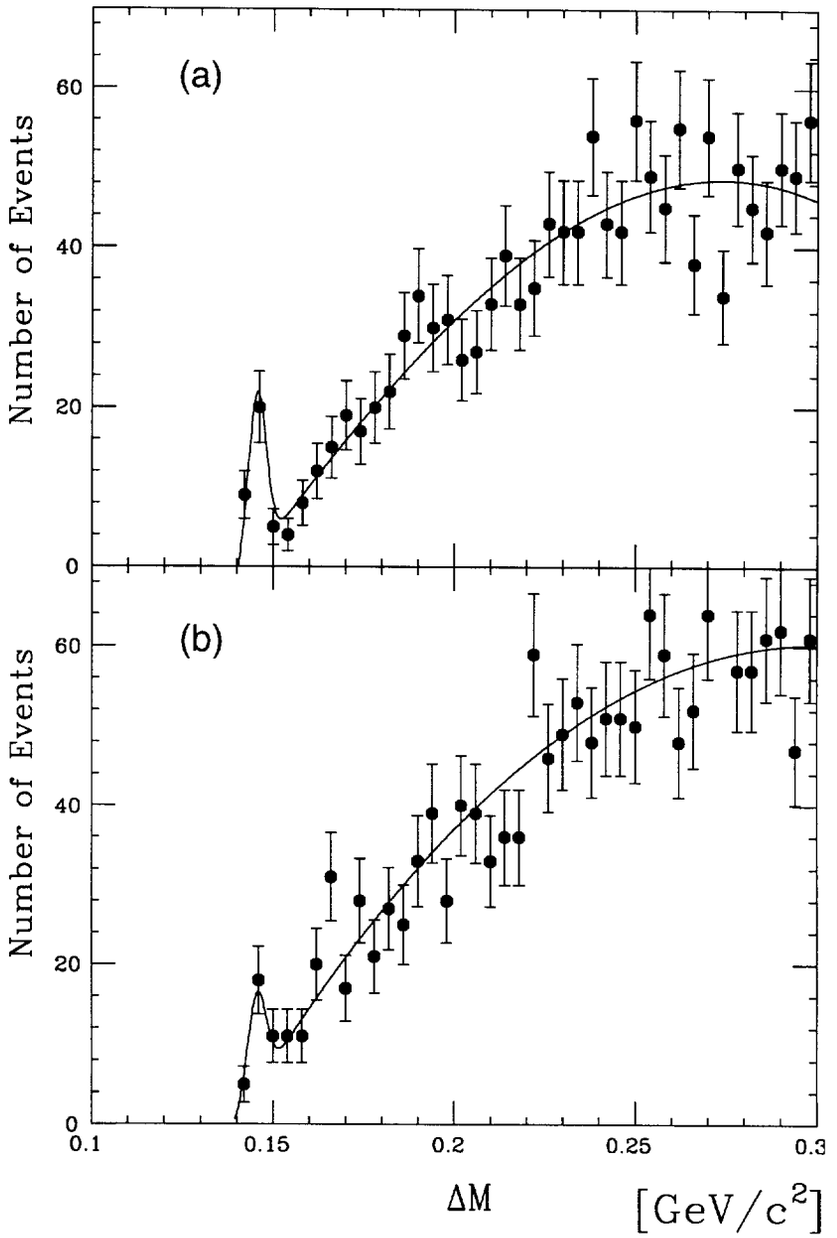

Figure 3: Mass-difference distributions in the $D^{*\pm} \rightarrow D^0\pi^\pm$, $D^0 \rightarrow K^\mp\pi^\pm$(a) and $D^0 \rightarrow K^\mp\pi^\pm\pi^\mp\pi^\pm$(b) branches. In each figure, the solid curve is the sum of the third-order polynomial function used to estimatefor the the backgrounds (see the text) and a Gaussian-shape signal.

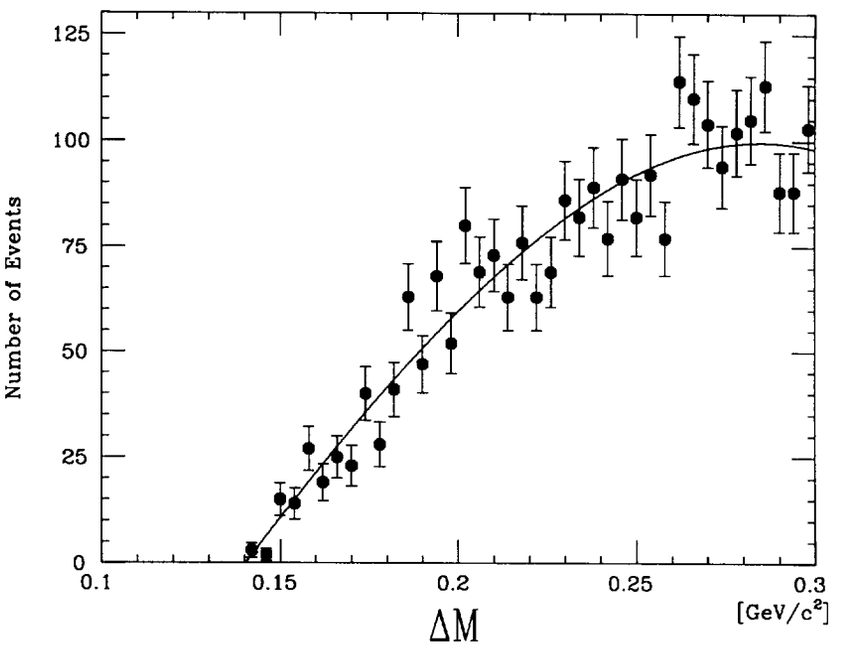

Figure 4: Mass-difference distribution for control samples in which the invariant mass of a $K^{\mp}\pi^{\pm}$ combination falls into the off-D^0 mass region (see text). The solid curve is the best fit to ΔM with a third-order polynomial function.

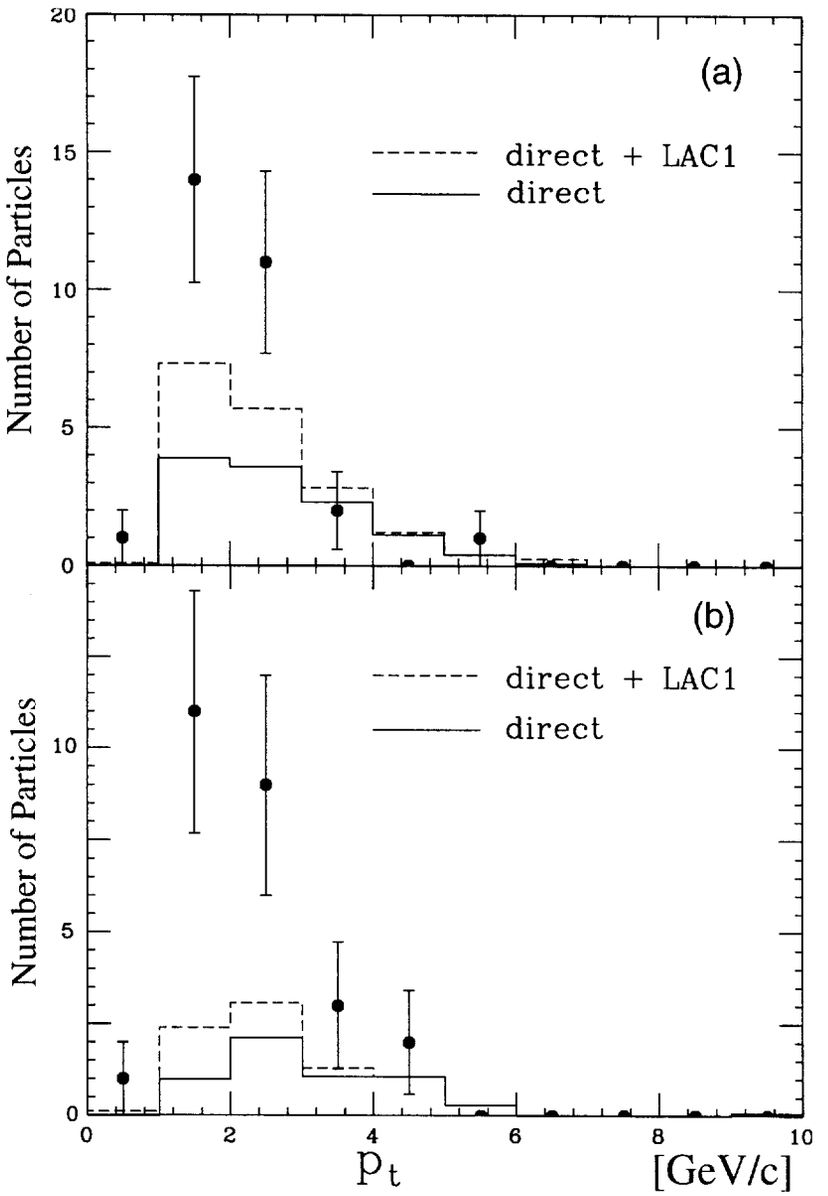

Figure 5: Transverse-momentum distributions of the $D^{*\pm}$ observed in the decay branches of $D^{*\pm} \to K^{\mp}\pi^{\pm}\pi^{\pm}$(a) and $D^{*\pm} \to K^{\mp}\pi^{\pm}\pi^{\mp}\pi^{\pm}\pi^{\pm}$(b). The closed circles are for $D^{*\pm}$ candidates, including the backgrounds (see text). The solid histogram shows the Monte-Carlo expectation for the direct process without a QCD correction, and the dashed histogram for the direct process + LAC1.

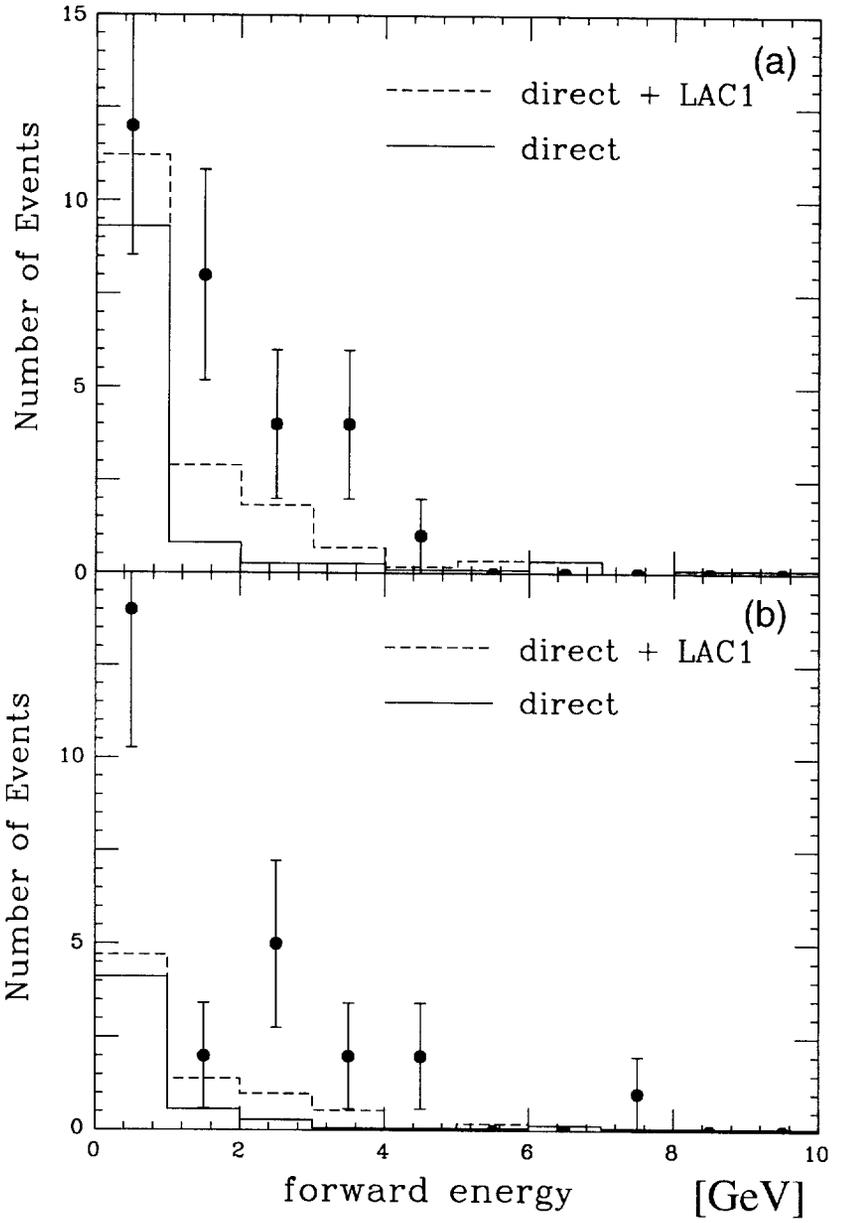

Figure 6: Distributions of the forward energy flow associated with the $D^{*\pm}$ events observed in the decay branches $D^{*\pm} \to K^{\mp}\pi^{\pm}\pi^{\pm}$(a) and $D^{*\pm} \to K^{\mp}\pi^{\pm}\pi^{\mp}\pi^{\pm}\pi^{\pm}$(b). The closed circles are the experimental data, including the backgrounds (see text). The solid and dashed histograms indicate the expectations for the direct process without a QCD correction and for the direct process + LAC1, respectively.